



Synthesis of wheat straw cellulose-g-poly (potassium acrylate)/PVA semi-IPNs superabsorbent resin



Jia Liu^a, Qian Li^{a,*}, Yuan Su^{a,b}, Qinyan Yue^a, Baoyu Gao^a, Rui Wang^a

^a Shandong Key Laboratory of Water Pollution Control and Resource Reuse, School of Environmental Science and Engineering, Shandong University, 250100 Jinan, PR China

^b School of Mathematic and Quantitative Economics, Shandong University of Finance and Economics, 250100 Jinan, PR China

ARTICLE INFO

Article history:

Received 5 June 2012

Received in revised form

25 December 2012

Accepted 17 January 2013

Available online 4 February 2013

Keywords:

Semi-IPNs superabsorbent resin

Wheat straw cellulose

Acrylic acid

Polyvinyl alcohol

Water absorbency

ABSTRACT

To better use wheat straw and minimize its negative impact on environment, a novel semi-interpenetrating polymer networks (semi-IPNs) superabsorbent resin (SAR) composed of wheat straw cellulose-g-poly (potassium acrylate) (WSC-g-PKA) network and linear polyvinyl alcohol (PVA) was prepared by polymerization in the presence of a redox initiating system. The structure and morphology of semi-IPNs SAR were characterized by means of FTIR, SEM and TGA, which confirmed that WSC and PVA participated in the graft polymerization reaction with acrylic acid (AA). The factors that can influence the water absorption of the semi-IPNs SAR were investigated and optimized, including the weight ratios of AA to WSC and PVA to WSC, the content of initiator and crosslinker, neutralization degree (ND) of AA, reaction temperature and time. The semi-IPNs SAR prepared under optimized synthesis condition gave the best water absorption of 266.82 g/g in distilled water and 34.32 g/g in 0.9 wt% NaCl solution.

© 2013 Elsevier Ltd. All rights reserved.

1. Introduction

Superabsorbent resin (SAR) is loosely cross-linked hydrophilic polymer with network structure, which has the ability to absorb and retain large amounts of aqueous fluids, and the absorbed solution cannot be released even under certain pressure. Based on these properties, SAR has been successfully applied in agriculture and horticulture to reduce irrigation frequency, and improve the physical properties of soil (Abedi-Koupai, Sohrab, & Swarbrick, 2008; Chu, Zhu, Li, & Huang, 2006). Semi-interpenetrating polymer networks (semi-IPNs) are characterized by the penetration on a molecular scale of networks by some of the linear or branched macromolecules (Sperling, 1984). Semi-IPN systems usually exhibit surprising properties superior to either of the two single polymer alone (Myung et al., 2008). Superabsorbents of semi-IPNs, which are composed of crosslinked and linear polymers can be used to enhance the performance of polymer composites.

Recently, SARs with excellent properties prepared by synthesis (Hua & Wang, 2009), starch (Keshava, Murali, Sreeramulu, & Mohana, 2006) and cellulose (Bao, Ma, & Li, 2011) have already been reported. Synthetic polymer SAR is difficult to biodegrade and starch grafted SAR has poor performance in mildew resistance, which restrict their application in agriculture. SAR based on

cellulose can overcome the disadvantages of them. Due to the abundant resources and enormous potential to reduce production cost, cellulose grafted SARs with eco-friendly property and biodegradability are found increasing interest in the academic and industrial field (Lionetto, Sannino, & Maffezzoli, 2005). Wheat straw (WS), as a by-product of grain crops, is an important biological resource in the crop production system (Talebnaia, Karakashev, & Angelidaki, 2010) and contains 40–60% natural cellulose. Wheat straw cellulose (WSC), which has a large amount of hydrophilic groups, can be used as the basic skeleton to synthesize SAR.

Polyvinyl alcohol (PVA) has been widely explored as a water-soluble polymer for numerous biomedical and pharmaceutical applications due to its advantages of non-toxic, non-carcinogenic, excellent chemical resistance and bioadhesive properties (Roberts, Bently, & Harris, 2002; Sahlin & Peppas, 1996). Moreover, PVA is also a biocompatible polymer that allows casting from water or organic solvents (Hirai, Muruyama, Suzuki, & Hayashi, 1992). So it is a suitable component for the preparation of semi-IPNs SAR and can enhance the mechanical toughness properties of SAR.

On the other hand, the growth of plants and their quality are mainly depended on the quantity of fertilizer and water. So researches in semi-IPNs superabsorbent have been contributed to the development of the superabsorbent containing fertilizer, such as N, P, K and humic substances (Guo, Liu, Zhan, & Wu, 2005; Liang, Liu, & Wu, 2007; Zhang, Liu, Li, & Wang, 2006). In this work, WS pretreated by ammonia can contain more nitrogen. Potassium hydroxide (KOH) was used as a neutralizing agent to neutralize

* Corresponding author. Tel.: +86 531 88361812; fax: +86 531 88364513.
E-mail address: qianli123sdu@yahoo.com.cn (Q. Li).

acrylic acid (AA) during the polymerization, which can make the superabsorbent rich in potassium and provide crops with potassium fertilizer.

In the present paper, a novel wheat straw cellulose-g-poly (potassium acrylate)/polyvinyl alcohol (WSC-g-PKA/PVA) semi-IPNs SAR, which was synthesized by graft copolymerization and semi-IPNs technology was studied. The introduction of the WSC-g-PKA/PVA semi-IPNs SAR was expected to provide a new way to extend the utilization of WS, what was more, to lower the cost of production and improve biodegradation property of semi-IPNs superabsorbents. It is expected that water absorbency of the new type SAR with improved structure and performance can be developed by the effective combination of WSC, AA and PVA. The WSC-g-PKA/PVA semi-IPNs SAR can be effectively used in agriculture as water retention material and improve the water retentivity of soil.

2. Experimental

2.1. Materials

Acrylic acid (AA, AR), polyvinyl alcohol (PVA, AR), N,N'-methylene-bis-acrylamide (MBA, AR), potassium persulfate ($K_2S_2O_8$, AR), ammonium cerium nitrate ($(NH_4)_2Ce(NO_3)_6$, AR), sodium sulfite (Na_2SO_3 , AR) and potassium hydroxide (KOH, AR) were all purchased from Dengke factory, Tianjin, China. Stock solutions of MBA (2.0 g/100 ml dist. water), PVA (15.0 g/250 ml dist. water) and the concentrations of all initiators were 2.0 g/100 ml dist. water.

2.2. Preparation of WSC-g-PKA/PVA semi-IPNs SAR

The washed and dried wheat straw were smashed and sifted through a 100-mesh sieve. Then the WS powder was soaked in 10% ammonia at the mass ratio of 1:12 for 48 h, washed with distilled water and filtered by a vacuum filter. The filtered residue was dipped in 1 mol/L nitric acid at a mass ratio of 1:12, and heated at 100 °C for 45 min. Then the mixture was washed and filtered by the same way. Finally, it dried at 70 °C to obtain WSC.

The semi-IPNs SARs were prepared by graft polymerization among AA, PVA and WSC in aqueous solution. 1.0 g WSC was put in a three-necked flask equipped with a stirrer. The water bath was heated slowly to 50 °C and maintained at this temperature. Stock solutions of $K_2S_2O_8$ and $(NH_4)_2Ce(NO_3)_6$ were added into the flask. After 15 min, Na_2SO_3 and monomer AA partially neutralized by KOH were successively added. AA and WSC were adequately polymerized. 15 min later, PVA was put in. Finally, MBA was added after 45 min. The same temperature and stirrer speed were maintained for 4 h. After the reaction, the formed semi-IPNs SARs were oven dried at 70 °C until to reach constant weight.

2.3. Characterization

The transformation infrared spectra (FTIR) of the WSC-g-PKA/PVA semi-IPNs SARs were recorded using a NEXUS-470 series FTIR spectrometer (Thermo Nicolet, NEXUS). The samples were powdered and mixed with KBr to make pellets. The morphological variation of the samples were examined with a Hitachi S-520 scanning electron microscope (Tokyo, Japan). Thermo gravimetric analysis (TGA) was performed on an analyzer with the temperature ranged from 10 to 600 °C. N_2 was used as the carrier gas with a 10 °C/min heating rate.

2.4. Measurement of swelling behavior and kinetics

In the experiment, 0.50 g samples were immersed in excess distilled water and 0.9 wt% NaCl aqueous solution, respectively, at room temperature for 5 h to reach swelling equilibrium. Then

swollen samples were filtered through a 100-mesh gauze to separate from unabsorbed water and weighted. The water absorption amount Q_{eq} (g/g) was calculated using the following equation:

$$Q_{eq} = \frac{M - M_0}{M_0} \quad (1)$$

where M_0 (g) and M (g) are the weights of the dry and swollen sample, respectively. Q_{eq} was calculated as grams of water per gram of sample. Water absorbency of the sample in both distilled water and 0.9 wt% NaCl solution were tested in the same way.

The swelling kinetics of WSC-g-PKA/PVA semi-IPNs SAR in distilled water was measured according to the following procedure: 0.50 g sample was immersed in 500 mL distilled water at set intervals (3, 5, 10, 15, 30, 45, 60, 75, 90, 120, 150, 180, 210 and 240 min), then swollen samples were filtered and the water absorption of SAR can be calculated according to Eq. (1). The swelling kinetics in 0.9 wt% NaCl solution was tested in the same way.

3. Results and discussion

3.1. FTIR results

The FTIR spectrums of WSC and WSC-g-PKA/PVA semi-IPNs SAR were shown in Fig. 1. From the FTIR spectrum of WSC, the absorption peaks at 3412 cm^{-1} , 2916 cm^{-1} and 1636 cm^{-1} were assigned to hydrogen bonded —OH stretching vibration, methylene and —OH stretching, respectively, which were characteristic absorptions in cellulose structures.

Compared with absorption peaks of WSC, the SAR revealed some changes of the characteristic spectra peaks, suggesting that the serial compositions of WSC had changed during the polymerization (Riyajan, Chaiponban, & Tanbumrung, 2009). The peak at 3443 cm^{-1} in SAR was larger than that of WSC, which was attributed to —OH stretching vibration of PVA. Furthermore, compared with WSC, the peaks observed between 1636 cm^{-1} (C=O of amide I band) and 1420 cm^{-1} (carbonyl stretch) were decreased in SAR. Due to the cross-linking reaction, peak at 1426 cm^{-1} (symmetric CH_2 bending vibration) was shifted to a lower wavenumber, 1414 cm^{-1} . And the intensity of this peak was also reduced. This shift indicated the development of new inter- and intra-molecular hydrogen bonds (Ciolacu, Kovac, & Kokol, 2010; Oh et al., 2005). However, three larger peaks appeared at 1566, 1414 and 1105 cm^{-1} were related to —COO[−] groups, C—O—C stretching and $\nu_{C=O}$ of AA, respectively. Specifically, —COOH groups in AA had transformed to —COO[−] groups (Zheng, Liu, & Wang, 2011). The peak at 1058 cm^{-1} ,

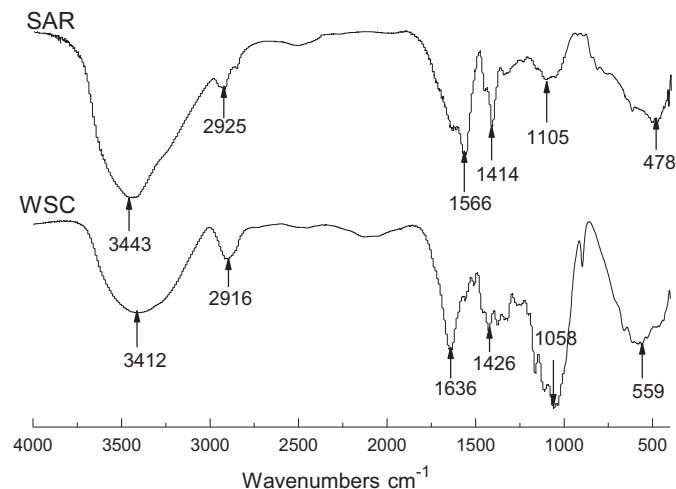


Fig. 1. FTIR spectra of WSC and WSC-g-PKA/PVA semi-IPNs SAR.

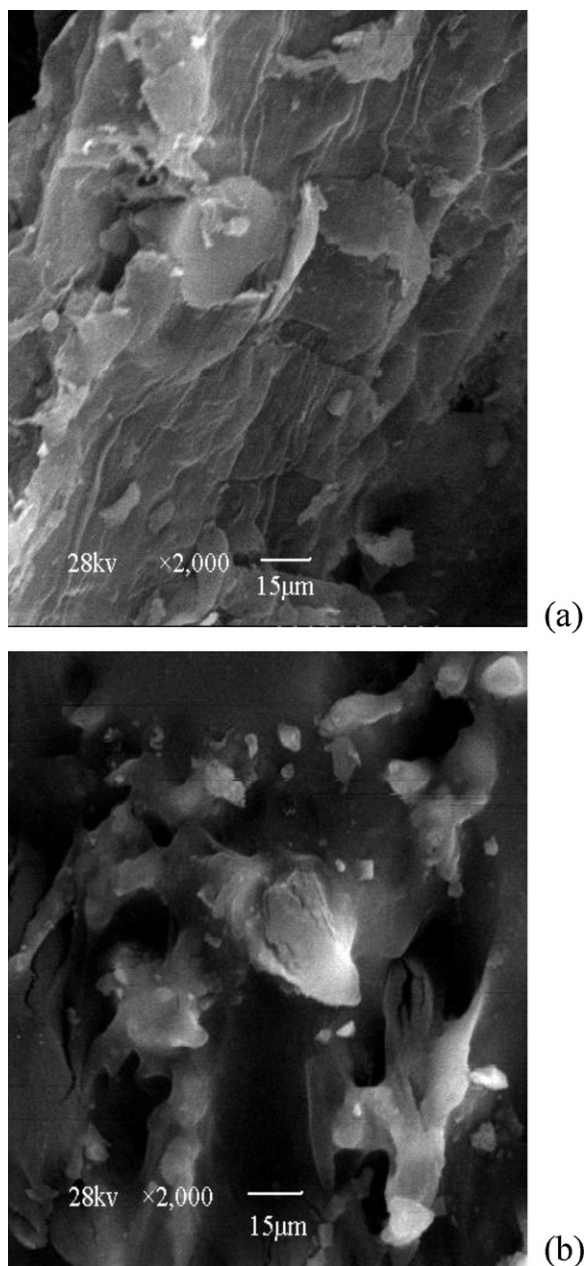


Fig. 2. SEM of WSC (a) and WSC-g-PKA/PVA semi-IPNs SAR (b).

assigned to C–O stretching vibration, disappeared from SAR spectrum as a result of cross-linking process. The weaker absorption peak at 559 cm^{-1} in SAR than in WSC, and the bending vibration observed at 478 cm^{-1} , suggested that the graft copolymerization between hydroxyl groups on WSC and AA occurred during the reaction (Li, Zhang, & Wang, 2007). Based on the information revealed in Fig. 1, it could obtain that grafting polymerization of AA onto WSC and further semi-interpenetrating with PVA occurred during the chemosynthesis, and the resulting product was a composite based on PKA incorporating with WSC and PVA.

3.2. SEM results

The scanning electron microscope (SEM) micrographs of both WSC and WSC-g-PKA/PVA semi-IPNs SAR were shown in Fig. 2 to compare the surface structure changes. As can be seen, WSC showed a smooth and dense surface, whereas WSC-g-PKA/PVA

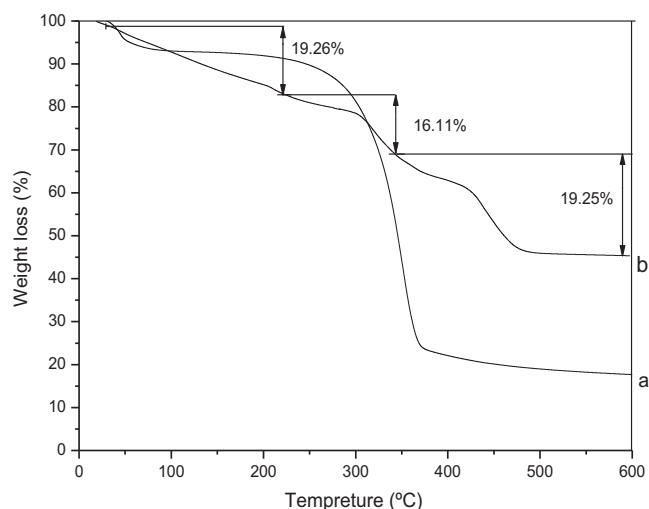


Fig. 3. TGA thermogram of WSC (a) and WSC-g-PKA/PVA semi-IPNs SAR (b).

semi-IPNs SAR exhibited a comparatively loose, coarse and porous surface. This coarse and improved surface was convenient for the penetration of water into the polymeric network (Liang, Yuan, Xi, & Zhou, 2009) and the enhancement of water absorption. This surface change might be ascribed to the removal and degradation of the cellulose particles and the formation of many irregular aggregates during graft copolymerization reaction. The different structures between WSC and WSC-g-PKA/PVA semi-IPNs SAR clearly indicated that graft copolymerization reaction was taken place between WSC and AA. Moreover, it revealed the combination of PVA, WSC and AA through semi-IPNs technology. From the SEM micrographs, it can be concluded that WSC-g-PKA/PVA semi-IPNs SAR was prepared.

3.3. TGA results

In order to understand and investigate the thermal behavior of WSC and WSC-g-PKA/PVA semi-IPNs SAR, both the samples were tested by TGA. From Fig. 3 it could be found that pure WSC showed a two-step thermogram, with the weight loss of 6.76% and 75.50%, respectively. The first stage occurred between 30 °C and 85 °C was due to the water evaporation. The major weight loss of WSC (a) was located at 315 °C and 354 °C, which was due to the degradation of cellulose in the graft copolymer. Comparatively speaking, WSC-g-PKA/PVA semi-IPNs SAR (b) had a mainly three-step thermogram, with the weight loss of 19.26%, 16.11% and 19.25%, respectively. The weight loss of the first stage was also corresponded to the water evaporation. The second stage occurred between 240 °C and 320 °C might be acceptable evidence for the decomposition of PVA and cellulose. To be more exact, it showed the decomposition of branches and side chain groups of the graft copolymer. The third stage occurred between 400 °C and 450 °C which was assigned to the main chain decomposition of the PVA and the main chain of the graft copolymer. The TGA results confirmed that the graft copolymerization reaction was taken place between WSC and AA, and then interpenetration between PVA and the grafted polymer occurred.

3.4. The effects of synthesis conditions on water absorbency of semi-IPNs SAR

3.4.1. Effect of weight ratios of AA to WSC and PVA to WSC on water absorbency of semi-IPNs SAR

The synthesis of WSC-g-PKA/PVA semi-IPNs SAR was mainly by the combination of WSC and AA, and then with PVA through

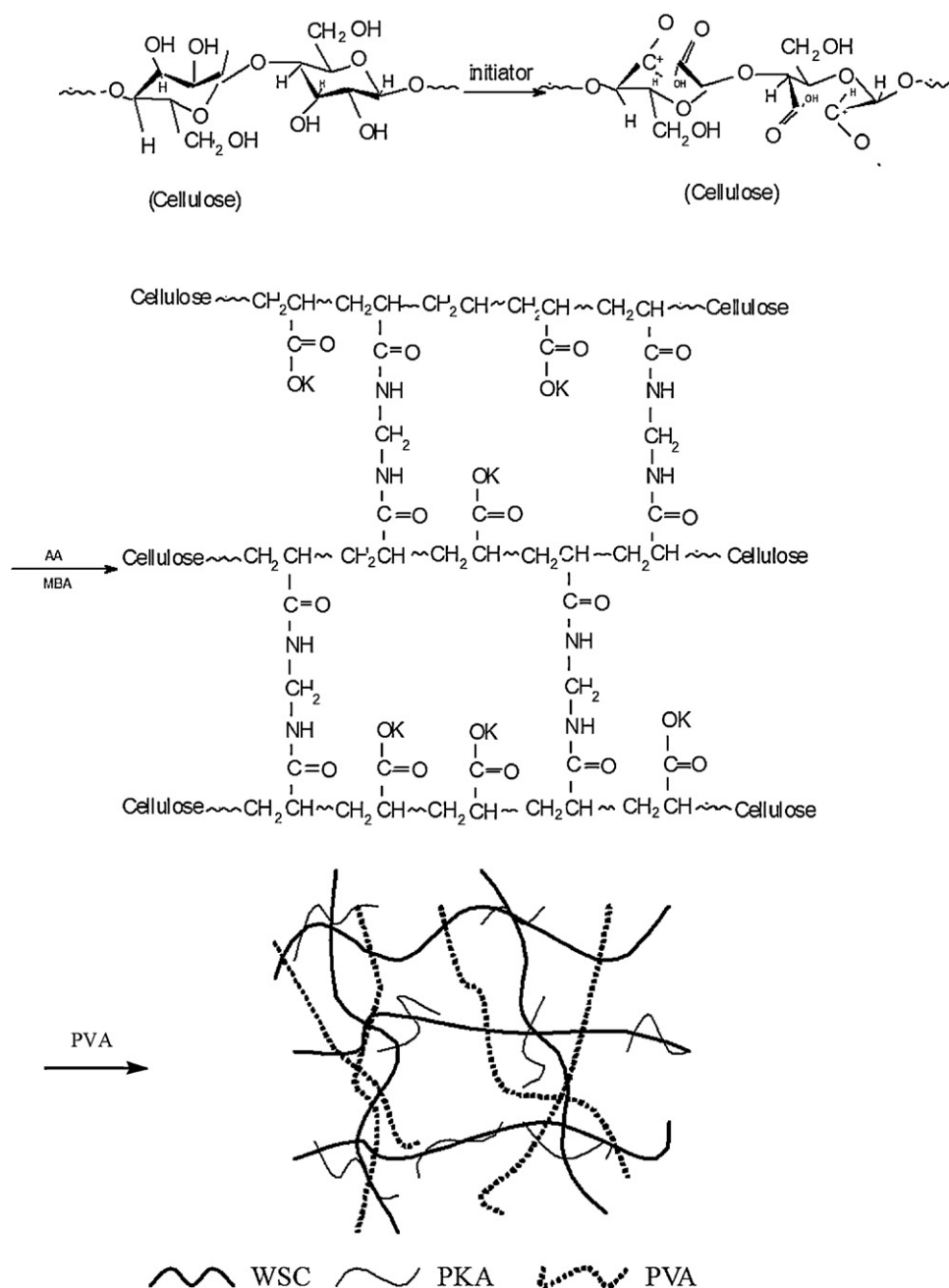


Fig. 4. Scheme of graft-copolymerization of WSC-g-PKA/PVA semi-IPNs SAR.

semi-IPNs technique. A schematic illustration of the preparation of WSC-g-PKA/PVA semi-IPNs SAR was shown in Fig. 4. As the basic skeleton, each cellulose unit could not be broken and the main reaction of the first step was activation. A large proportion of the reaction function groups, such as $-\text{COOH}$ groups in AA, $-\text{CH}_2$ and $-\text{OH}$ groups in cellulose could be grafted in the second step, resulting in the ratio of graft was about 70% (Singha & Rana, 2012). For the convenience of study, as the only monomer, AA was used as the reference. The effects of weight ratios of AA to WSC and PVA to WSC on water absorbency of SAR were shown in Table 1. It was clear that with the increase of weight ratios of AA to WSC from 6 to 10 and PVA to WSC from 1 to 2, the water absorbency of SAR in distilled water and 0.9 wt% NaCl solution increased from 107.16 to 244.66 g/g and 18.64 to 28.48 g/g, respectively. The optimized weight ratios of AA to WSC and PVA to WSC were 10:1 and 2:1, respectively. It could be concluded that with the increase of AA content, more AA molecules

grafted onto the skeleton of WSC, increasing the hydrophilicity and water absorbency of SAR. Concretely, more hydrophilic groups such as $-\text{OH}$, $-\text{COO}^-$ and $-\text{COOH}$ were grafted onto the WSC, which was favorable to the water absorption. PVA contained nonionic hydrophilic groups, such as $-\text{OH}$. Therefore, with the increase of PVA content, more PVA would react with WSC-g-PKA during the polymerization process and improved the polymeric network, so enhanced the water absorption ability. However, when the amount of monomer AA was high, the network of polymer became closer and the superfluous AA turned to be PKA homopolymer. So, soluble materials at fixed cross-linking density (Finkenstadt & Willett, 2005) increased and the expansion of net structure and the movement of free radicals were restricted, which resulted in the drop of water absorbency. Meanwhile, when PVA content was too high, there would be less $-\text{COO}^-$, and the water absorption could be decreased. Specifically, more PVA were generated in the polymeric

Table 1

Effects of AA, PVA, initiator, MBA, ND of AA, temperature and time on water absorbency of semi-IPNs SAR.

Various conditions in synthesis		The water absorbency in distilled water (g/g)	The water absorbency in 0.9 wt% NaCl solution (g/g)
The weight ratio of AA (g) to WSC (g)	6:1	107.16	18.64
	8:1	157.44	21.34
	10:1	246.66	28.48
	12:1	186.54	27.12
	14:1	165.28	22.26
The weight ratio of PVA (g) to WSC (g)	1:1	170.20	22.06
	1.5:1	225.12	23.64
	2:1	239.66	28.12
	2.5:1	194.32	24.14
	3:1	159.26	21.42
The weight ratio of $K_2S_2O_8$ to AA (%)	0.5	89.10	16.34
	1	122.14	20.42
	1.5	181.60	27.90
	2	206.48	30.58
	2.5	177.64	26.86
	3	176.82	25.96
The weight ratio of MBA to AA (%)	0.2	143.26	20.14
	0.4	212.38	27.24
	0.6	190.64	24.36
	0.8	156.82	22.22
	1.0	139.84	20.12
	1.2	118.10	18.34
Neutralization degree of AA (%)	55	190.64	22.36
	65	225.38	29.80
	75	189.04	23.24
	85	174.68	22.16
	95	147.62	19.76
Temperature ($^{\circ}C$)	30	172.10	21.78
	40	189.62	24.88
	50	266.82	34.32
	60	240.76	32.46
	70	212.14	28.56
Time (h)	3	150.90	21.76
	4	214.24	27.82
	5	182.52	23.44
	6	176.36	23.12

network and therefore the osmotic pressure between the polymeric network and external solution decreased (Liu, Miao, & Wang, 2009), resulting the apparent decrease of water absorbency.

3.4.2. Effect of initiator content on water absorbency of semi-IPNs SAR

The three initiators, i.e. $K_2S_2O_8$, Na_2SO_3 and $(NH_4)_2Ce(NO_3)_6$ were combined to form a oxidation and reduction system. The best mass ratios between the three initiators were $m(K_2S_2O_8):m(Na_2SO_3)=3:1$ and $m((NH_4)_2Ce(NO_3)_6):m(K_2S_2O_8)=1:5$ (Guo, Li, & Li, 2006). In this work, it used the weight change of $K_2S_2O_8$ to study the effect of initiator content on water absorbency of semi-IPNs SAR. As can be seen in Table 1, as the weight ratio of $K_2S_2O_8$ to AA increased from 0.5 to 2 wt%, the water absorbency in distilled water and 0.9 wt% NaCl solution increased from 89.10 to 206.48 g/g and from 16.34 to 30.58 g/g, respectively, and then decreased with further weight ratio increase. The change of the water absorbency of the semi-IPNs SAR with the increase of the amount of $K_2S_2O_8$ was related to the relationship between average chain length and concentration of the initiator in the polymerization (Zhang, Wang, & Wang, 2009). When the dosage of initiator was low, free radicals of cellulose molecules could not be fully produced and the polymerization was tardive, which led to less grafted points and grafted monomer amount. As a result, effective three-dimensional polymer network could not be formed, which might result in low water absorbency. With the increase of the initiator content, more graft polymerization occurred between AA and WSC, leading to the

formation of more stable network structures and contributed to the enhancement of water absorbency. When the amount of the initiator was too high, a strong reaction with the cellulose molecular occurred, which could produce more free radicals and the cross-linking density was high. As a result, more AA molecules were grafted with the cellulose molecules and the main polymer chain length was shortened. Consequently, the water absorbency of semi-IPNs SAR dropped.

3.4.3. Effect of cross-linker content on water absorbency of semi-IPNs SAR

The relationship between water absorbency and cross-linking density can be explained by Flory's network theory. Based on the theory, water absorbency of superabsorbents is mainly affected by cross-linking density. The effect of MBA content, which was used as the cross-linker in the polymerization on water absorbency of semi-IPNs SAR was shown in Table 1. As can be seen from the table, the water absorbency increased with the increase of cross-linker content from 0.2 to 0.4 wt% and then decreased. This was largely due to the fact that cross-linking density was likely to increase alongside increasing content of MBA. When the weight ratio of MBA to AA was lower than 0.4 wt%, the cross-linking density was low which resulted in the decreasing of the gel strength of semi-IPNs SAR. Semi-IPNs SAR would become water soluble resin after water absorbed. So the water absorption was low. As the cross-linking density increasing, more three-dimensional polymer network with small aperture formed, which would contribute to

the water absorbency of semi-IPNs SAR. However, when the cross-linker content was too high, the crosslinking density would be high and the apertures in three dimensional networks became smaller, and the elasticity of the polymeric network of the superabsorbent decreased, which led to the decrease of water absorbency.

3.4.4. Effect of neutralization degree of AA on water absorbency of semi-IPNs SAR

The neutralization degree (ND) of AA is also an important factor on the absorbency of SAR. The effect of ND of AA, which was neutralized by KOH, was shown in Table 1. The water absorbency increased with the increase of the ND of AA until to 65% and then showed a downward trend when above 65%. The colloid elasticity, ionic osmotic and affinity of polymer toward water had an influence on the swelling ability and absorbency of SAR, according to previous works (Pourjava & Amini-Fazl, 2007). When the ND was low, the acidity of water phase was high and the polymerization was quickly completed, which consequently led to the formation of highly cross-linked polymers and caused low water absorbency. With the increase of ND, on one hand, the speed of reaction was slowed down and the self-crosslinking degree of AA was reduced; on the other hand, more hydrophilic groups grafted on the chain of the composite and the amount of K^+ rose, which resulted in the enhancement of ionic strength and the inside osmotic pressure of cross-linking network. Both of them could contribute to the increase of water absorbency. However, if the ND of AA was above 65%, more K^+ ions in the polymeric network would react with the $-COO^-$ group, resulting in the reduction of void space caused by mutual repulsion of $-COO^-$ groups. Furthermore, branched chains of small molecules turned longer which blocked the mesh of SAR and restricted the expansion of the mesh structure. Consequently, the water absorbency of SAR dropped.

3.4.5. The effect of reaction temperature on water absorbency of semi-IPNs SAR

The effect of reaction temperature on the water absorbency was studied by preparing a series of SAR at different temperatures and the results were shown in Table 1. At lower temperatures, graft polymerization reaction was slow and grafted yield was low, which hampered the formation of three-dimensional polymer network. With the increase of temperature, the molecular would obtain more activation energy and consequently both the chain initiation and chain growth of polymerization reaction were accelerated. So, the grafting copolymerization reaction was enhanced, which would lead to higher grafted yield and water absorption capacity. However, when the temperature was too high, the reaction rate would increase substantially even resulted in violent polymerization. As a result, a lot of monomer groups would graft to the main chain and led to a close network structure, which was not helpful for water absorption. Meanwhile, many side effects between the monomers would happen at higher temperature and the by-products would have a bad effect on the water absorption (Ma, Li, & Yue, 2011). So the optimized reaction temperature was 50 °C.

3.4.6. The effect of reaction time on water absorbency of semi-IPNs SAR

The effect of reaction time on water absorbency was shown in Table 1. As can be seen from the table, the water absorbency increased along with the increase of the reaction time and the optimized time was 5 h. This was ascribed to the fact that when the reaction time was short, grafted polymerization reaction was not complete. As the time increasing, more cross-linking reaction happened and promoted the formation of more network structure. However, overlong reaction time would result in many branched chains in the network structure, which would intertwine with each

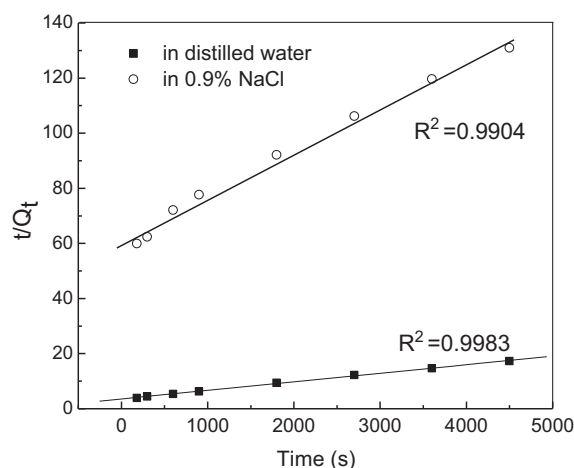


Fig. 5. Swelling kinetic curves of WSC-g-PKA/PVA semi-IPNs SAR in distilled water and 0.9 wt% NaCl solution.

other and obstruct the expansion of the resin mesh structure. So the water absorbency showed a decrease above the optimum time.

3.4.7. Swelling kinetics

The swelling kinetics of WSC-g-PKA/PVA semi-IPNs SAR in distilled water and 0.9 wt% NaCl were evaluated by Schott's pseudo second order kinetics model (Schott, 1992).

$$\frac{t}{Q_t} = \frac{1}{K_{is}} + \left(\frac{1}{Q_{\infty}} \right) t \quad (3)$$

where Q_t (g/g) was the water absorption of SAR at time t ; Q_{∞} (g/g) was the theoretical equilibrium swelling capacity; K_{is} was the initial swelling rate constant (g/g s). As can be seen in Fig. 5, the plot of t/Q_t versus t gave straight lines and the linear correlation coefficients of the lines were 0.9983 and 0.9904, respectively. The results indicated that the pseudo second order model could be effectively used to evaluate swelling kinetics of SAR. Q_{∞} and K_{is} of SAR can be calculated by the slope and intercept of each fitted straightened line. Q_{∞} values were 322.58 g/g and 49.3496 g/g, K_{is} were 0.2806 g/g s and 0.0165 g/g s in distilled water and 0.9 wt% NaCl solution, respectively. It can be concluded that the swelling capacity and swelling rate in distilled water were much higher than in 0.9 wt% NaCl solution.

3.5. An orthogonal experiment

Orthogonal experimental design is a widely used method in the tests which orthogonally selects the representative dots from the overall ones. The orthogonal experimental design is the main method of the fractional factorial design which can comprehensively reflect the influence of all the factors selected in the tests, and has been used in many research domains for its high efficiency, speediness and economy.

In order to verify and sift out the optimal condition, an orthogonal experiment with four factors and three levels was designed. Four variables, i.e. the weight ratio of AA to WSC, the weight ratio of PVA to WSC, ND of AA and weight ratio of $K_2S_2O_8$ to AA were considered to be the important factors (Zheng et al., 2011). Nine synthesis conditions were carried out at weight ratio of AA to WSC 8, 10 and 12, weight ratio of PVA to WSC 1.5, 2 and 2.5, ND of AA 55%, 65% and 75%, weight ratio of $K_2S_2O_8$ to AA 1.5%, 2% and 2.5%. All selected factors were examined using an orthogonal $L_9(3)^4$ test presented in Table 2, with water absorbency in distilled water (Q_1) and water absorbency in 0.9 wt% NaCl solution (Q_2) as indexes. The orthogonal tests were designed and analyzed by the software of Orthogonal Design Assistant II, v3.1.

Table 2

Optimal reaction conditions determined by orthogonal tests.

Sample	A ^a (g)	B ^b (g)	C ^c (%)	D ^d (%)	Q ₁ ^e (g/g)	Q ₂ ^f (g/g)
1	8	1.5	1.5	55	144.56	20.36
2	8	2	2	65	224.76	27.74
3	8	2.5	2.5	75	167.52	23.84
4	10	1.5	2	75	193.40	24.16
5	10	2	2.5	55	259.12	33.46
6	10	2.5	1.5	65	227.28	26.68
7	12	1.5	2.5	65	273.46	29.52
8	12	2	1.5	75	242.44	25.68
9	12	2.5	2	55	304.92	37.14

^a The weight ratio of AA to WSC.^b The weight ratio of PVA to WSC.^c The weight ratio of K₂S₂O₈ to AA.^d ND of AA.^e Water absorbency in distilled water.^f Water absorbency in 0.9 wt% NaCl solution.**Table 3**Orthogonal L₉ (3)⁴ test analysis.

	A		B		C		D	
	Q ₁	Q ₂	Q ₁	Q ₂	Q ₁	Q ₂	Q ₁	Q ₂
k ₁ ^a	178.947	23.98	203.807	24.68	204.760	24.24	236.200	30.30
k ₂	226.600	28.08	242.107	28.94	241.027	29.68	241.833	27.98
k ₃	273.607	30.78	233.240	29.22	233.367	28.92	201.120	24.56
R ^b	94.660	6.80	38.300	4.54	36.267	5.44	40.713	5.74

^a Mean values of each factor in different levels.^b Extremum of each factor.

It was observed from Table 2 that the parameters of the high-est Q₁ and Q₂ were 304.92 g/g and 37.14 g/g (No. 9), respectively, which were obvious among all the designed orthogonal tests from No. 1 to No. 9. Compared results of orthogonal test with that of the single factor experiments, all the optimal synthesis conditions were the same except the weight ratio of AA to WSC. It was indicted that at the condition of $m(\text{AA}):m(\text{WSC}) = 12$, the water absorbency of SAR in both distilled water and 0.9 wt% NaCl solution was higher than other conditions. Taking into account of reducing the dosage of reactants and making the most of them, thereby the optimal synthesis conditions for WSC-g-PKA/PVA semi-IPNs SAR preparation can be concluded as $m(\text{AA}):m(\text{WSC}) = 10$, $m(\text{PVA}):m(\text{WSC}) = 2$, $m(\text{K}_2\text{S}_2\text{O}_8):m(\text{AA}) = 2\%$, ND of AA 65%. Under this condition, the water absorbency in both distilled water and 0.9 wt% NaCl solution reached the maximum value.

A further orthogonal analysis (Table 3) was warranted to determine the key influential factor. The results of experiments presented in Table 3 indicated that the most outstanding effect factor on the water absorption performance of semi-IPNs SAR was the weight ratio of AA to WSC. The influence of each factor on the water absorbency of WSC-g-PKA/PVA semi-IPNs SAR was decreased in the order: the weight ratio of AA to WSC > ND of AA > the weight ratio of PVA to WSC > the weight ratio of K₂S₂O₈ to AA in distilled water and the weight ratio of AA to WSC > ND of AA > the weight ratio of K₂S₂O₈ to AA > the weight ratio of PVA to WSC in 0.9 wt% NaCl solution, respectively, according to the R values. The weight ratio of AA to WSC was found to be the most important determinant in the preparation of WSC-g-PKA/PVA semi-IPNs SAR for its markedly high R value than other influential factors.

4. Conclusions

A series of WSC-g-PKA/PVA semi-IPNs superabsorbent resins were synthesized by free-radical graft copolymerization and semi-interpenetration through WSC and AA in the presence of PVA

in aqueous solution. Structure and properties of SAR were analyzed by FTIR, SEM and TGA, the results of which confirmed the occurrence of copolymerization process. It was found that the optimum condition was that the weight ratio among the WS, AA and PVA was $m(\text{WS}):m(\text{AA}):m(\text{PVA}) = 1:10:2$, reaction temperature 50 °C, reaction time 5 h, neutralization degree of AA 65%. The maximum water absorbency of semi-IPNs was 266.82 g/g in distilled water and 34.32 g/g in 0.9 wt% NaCl solution. The Schott's pseudo second order kinetics model presented high coefficient of determination in distilled water and 0.9 wt% NaCl solution, which provided evidence for future study. This paper was an effort to develop new kind of SAR with improved structure and environmental friendly property and also provided a new way to expand the utilization of wheat straw to product superabsorbent material.

Acknowledgements

The authors are grateful to the support of the National Natural Science Foundation of China (21007034), Natural Science Foundation of Shandong Province (ZR2010EQ031) and Foundation for Young Excellent Scientists of Shandong Province (BS2009NY005).

References

- Abedi-Koupai, J., Sohrab, F., & Swarbrick, G. (2008). Evaluation of hydrogel application on soil water retention characteristics. *Journal of Plant Nutrition*, 31, 317–331.
- Bao, Y., Ma, J. Z., & Li, N. (2011). Synthesis and swelling behaviors of sodium carboxymethyl cellulose-g-poly(AA-co-AM-co-AMPS)/MMT superabsorbent hydrogel. *Carbohydrate Polymers*, 84, 76–82.
- Chu, M., Zhu, S. Q., Li, H. M., & Huang, Z. B. (2006). Synthesis of poly(acrylic acid)/sodium humate superabsorbent composite for agricultural use. *Applied Polymer Science*, 102, 5137–5143.
- Ciolacu, D., Kovac, J., & Kokol, V. (2010). The effect of the cellulose-binding domain from Clostridium cellulovorans on the supramolecular structure of cellulose fibers. *Carbohydrate Research*, 345, 621–630.
- Finkenstadt, V. L., & Willett, J. L. (2005). Reactive extrusion of starch–polyacrylamide graft copolymer: Effects of monomer/starch ratio and moisture content. *Macromolecular Chemistry and Physics*, 206, 1648–1652.
- Guo, M. Y., Liu, M. Z., Zhan, F. L., & Wu, L. (2005). Preparation and properties of a slow-release membrane-encapsulated urea fertilizer with superabsorbent and moisture preservation. *Industrial and Engineering Chemistry Research*, 44, 4206–4211.
- Guo, Y., Li, X., & Li, C. (2006). Preparation of agricultural superabsorbent resin by wheat straw. *Fine Chemistry*, 23, 31–36.
- Hirai, T., Muruyama, H., Suzuki, T., & Hayashi, S. (1992). Imaging by Moiré patterns between similar polymer sheets of microconvex lenses closely arranged in a regular triangle pattern. *Applied Polymer Science*, 45, 1849–1852.
- Hua, S. B., & Wang, A. Q. (2009). Synthesis, characterization and swelling behaviors of sodium alginate-g-poly(acrylic acid)/sodium humate superabsorbent. *Carbohydrate Polymers*, 75, 79–84.
- Keshava, M. P. S., Murali, M. Y., Sreeramulu, J., & Mohana, R. K. (2006). Semi-IPNs of starch and poly(acrylamide-co-sodium methacrylate): Preparation, swelling and diffusion characteristics evaluation. *Reactive and Functional Polymers*, 66, 1482–1493.
- Li, A., Zhang, J. P., & Wang, A. Q. (2007). Utilization of starch and clay for the preparation of superabsorbent composite. *Bioresource Technology*, 98, 327–332.
- Liang, R., Liu, M. Z., & Wu, L. (2007). Controlled release NPK compound fertilizer with the function of water retention. *Reactive and Functional Polymers*, 67, 769–779.
- Liang, R., Yuan, H. B., Xi, G. X., & Zhou, Q. X. (2009). Synthesis of wheat straw-g-poly(acrylic acid) superabsorbent composites and release of urea from it. *Carbohydrate Polymers*, 77, 181–187.
- Lionetto, F., Sannino, A., & Maffezzoli, A. (2005). Ultrasonic monitoring of the network formation in superabsorbent cellulose based hydrogels. *Polymer*, 46, 1796–1803.
- Liu, Z., Miao, Y., & Wang, Z. (2009). Synthesis and characterization of a novel superabsorbent based on chemically modified pulverized wheat straw and acrylic acid. *Carbohydrate Polymers*, 77(1), 131–135.
- Ma, Z. H., Li, Q., & Yue, Q. Y. (2011). Synthesis and characterization of a novel superabsorbent based on wheat straw. *Bioresource Technology*, 102, 2853–2858.
- Myung, D., Waters, D., Wiseman, M., Duhamel, P. E., Noolandi, J., & Ta, C. N. (2008). Progress in the development of interpenetrating polymer network hydrogels. *Polymers for Advanced Technologies*, 19, 647–657.
- Oh, S. Y., Yoo, D. II., Shin, Y., Kim, H. C., Kim, H. Y., & Chung, Y. S. (2005). Crystalline structure analysis of cellulose treated with sodium hydroxide and carbon dioxide by means of X-ray diffraction and FTIR spectroscopy. *Carbohydrate Research*, 340(15), 2376–2391.

- Pourjava, A., & Amini-Fazl, M. S. (2007). Optimized synthesis of carrageenangraft-poly (sodium acrylate) super-absorbent hydroxyl using the Taguchi method and investigation of its metal ion absorption. *Polymer International*, 56(2), 283–289.
- Riyajan, S., Chaiponban, S., & Tanbumrung, K. (2009). Investigation of the preparation and physical properties of a novel semi-interpenetrating polymer network based on epoxised NR and PVA using maleic acid as the crosslinking agent. *Chemical Engineering Journal*, 153, 199–205.
- Roberts, M. J., Bently, M. D., & Harris, J. M. (2002). Chemistry for peptide and protein pegylation. *Advanced Drug Delivery Reviews*, 54, 459–476.
- Sahlin, J. J., & Peppas, N. A. (1996). Hydrogels as mucoadhesive and bioadhesive materials: A review. *Biomaterials*, 16, 1553–1561.
- Schott, H. (1992). Swelling kinetics of polymers. *Journal of Macromolecular Science B*, 31, 1–9.
- Singha, A. S., & Rana, R. K. (2012). Functionalization of cellulosic fibers by graft copolymerization of acrylonitrile and ethyl acrylate from their binary mixtures. *Carbohydrate Polymers*, 87, 500–511.
- Sperling, L. H. (1984). Interpenetrating polymer networks and related materials. *Polymer*, 18, 3593–3595.
- Talebna, F., Karakashev, D., & Angelidaki, I. (2010). Production of bioethanol from wheat straw: An overview on pretreatment, hydrolysis and fermentation. *Biore-source Technology*, 101(13), 4744–4753.
- Zhang, J. P., Liu, R. F., Li, A., & Wang, A. Q. (2006). Preparation, swelling behaviors, and slow-release properties of a poly(acrylic acid-co-acrylamide)/sodium humate superabsorbent composite. *Industrial and Engineering Chemistry Research*, 45, 48–53.
- Zhang, J., Wang, Q., & Wang, A. (2009). Synthesis and characterization of chitosan-g-poly (acrylic acid)/attapulgit super-absorbent composites. *Carbohydrate Polymers*, 68(2), 367–374.
- Zheng, Y., Liu, Y., & Wang, A. Q. (2011). Fast removal of ammonium ion using a hydrogel optimized with response surface methodology. *Chemical Engineering Journal*, 171, 1201–1208.